Journal of Materials Chemistry A

Accepted Manuscript

ROYAL SOCIETY OF CHEMISTRY

www.rsc.org/materialsA

Journal Name

RSCPublishing

ARTICLE

Cite this: DOI: 10.1039/x0xx00000x

Improvement of hydrogen evolution under visible light over $Zn_{1-2x}(CuGa)_xGa_2S_4$ photocatalysts by synthesis utilizing a polymerizable complex method

Ciro Scheremeta Quintans,[a] Hideki Kato,*[a] Makoto Kobayashi,[a] Hiroshi Kaga,[b] Akihide Iwase,[b,c] Akihiko Kudo[b,c] and Masato Kakihana[a]

Received 00th January 2012,
Accepted 00th January 2012

DOI: 10.1039/x0xx00000x

www.rsc.org/

Single phase $Zn_{1-2x}(CuGa)_xGa_2S_4$ was successfully synthesized by a two-step route: synthesis of an oxide precursor by a polymerizable complex (PC) method followed by sulfurization under a H_2S-Ar flow. The samples thus obtained were porous aggregates consisting of fine crystals with 50 nm of size. Among the examined compositions, $Zn_{0.4}(CuGa)_{0.3}Ga_2S_4$ (x = 0.3), showed the highest activity for H_2 evolution from an aqueous solution containing S^{2-} and SO_3^{2-} as electron donors under visible light irradiation. The apparent quantum yield of the optimized sample with deposition of 2 wt% of Rh was 19% at 420 nm. This value is higher than that of the sample synthesized by a solid state reaction (15%). Therefore, improvement of photocatalytic performance of $Zn_{0.4}(CuGa)_{0.3}Ga_2S_4$ for H_2 evolution has been achieved by using the two-step synthesis method including the preparation of an oxide precursor by the PC method.

1. Introduction

Ever since Honda-Fujishimas's major breakthrough of observing photoelectrochemical water splitting, [1] many studies have been done on searching for new photocatalyst materials and on improvements of their performances.[2–8] In the case of overall water splitting by powder photocatalysts, some materials, such as $NaTaO_3$:La,[9] Ga_2O_3:Zn,[10] can achieve really high quantum yields. However, these photocatalysts are active only under ultraviolet (UV) light. The amount of energy received from the sun in the UV range corresponds to only 4% of the total energy, while 46% of the light energy is in the visible range. Therefore, the development of visible-light-driven photocatalysts and improvement of those performances are important subjects.[11] In recent decades, many materials in wide categories, such as oxides,[12–18] oxynitrides,[19–22] carbon nitrides[23–25] and sulfides,[26–45] have been studied as visible-light-driven photocatalysts capable of H_2 evolution.

To date, several sulfide photocatalysts with the response to visible light have been developed by a concept of solid solutions between semiconductors with wide and narrow band gaps. A material possessing a conduction band (CB) at high potential is favoured as one end member in the solid solution. Therefore, making valence bands (VB) at a shallow position is indispensable to obtain visible-light-driven photocatalysts capable of H_2 production. Regarding this aspect, significant effects of Ag(I) and Cu(I) on narrowing band gaps have been described in several cases employing ZnS as a wide band gap material, such as $(AgIn)_xZn_{2(1-x)}S_2$, $(CuIn)_xZn_{2(1-x)}S_2$ and ZnS-$CuInS_2$-$AgInS_2$.[26–30] While CB and VB of ZnS consist of Zn4s4p and S3p orbitals, respectively, incorporation of Ag(I) and/or Cu(I) raises the VB potential due to the hybridization of the S3p and Ag4d and/or Cu3d orbitals.[26–36] These photocatalysts exhibit high activity for H_2 evolution from an aqueous solution containing suitable electron donors such as S^{2-} and SO_3^{2-}. The effects of Ag(I) and Cu(I) on narrowing the band gaps have been also shown in other materials, such as $(Cu,Ag)_2Zn(Ge,Sn)S_4$, $CuGa_2In_3S_8$, $AgGa_2In_3S_8$, $CuGa_3S_5$ and $Zn_{1-2x}(CuGa)_xGa_2S_4$.[32–34, 40]

Kakihana and Domen are pioneers who have achieved an improvement of photocatalytic activity using a polymerizable complex (PC) method, which is a solution-based method to obtain fine particles of complex oxides with high homogeneity, instead of a conventional solid state reaction (SSR) to synthesize oxide photocatalysts.[46] Synthesis by the PC method results in better materials with superior characteristics, such as fine particles, large surface areas, and the less crystalline defects which behave as recombination centers between photogenerated electrons and holes.[2]

As mentioned above, some sulfide solid solutions containing Ag(I) and/or Cu(I) are highly active photocatalysts for H_2 evolution. However, most of them are synthesized by SSR, which might not be the optimized approach. There are several homogeneous methods to prepare sulfides which lead to higher performance[47-50], however these methods are usually limited to simple sulfides such as CdS and ZnS. Few homogeneous methods have been reported for synthesis of complex sulfides.[51] In this scenario, developments of new synthetic approaches are important to improve performance. Among the sulfide solid solutions, $Zn_{1-2x}(CuGa)_xGa_2S_4$ has a promising potential for testing new synthesis techniques, due to its complex composition, easiness to tune the band gap accordingly with its composition in addition to a higher apparent quantum yield (15% at 420 nm[40]) than another ZnS-based solid solution $Zn_{0.5}Cd_{0.5}S$ (9.6%) containing toxic Cd.[45]

In this work, we examined the synthesis of $Zn_{1-2x}(CuGa)_xGa_2S_4$ photocatalysts through a two-step route, which involves the preparation of a highly homogeneous oxide precursor by the PC method and subsequent sulfurization of it, with the aim of improvement of photocatalytic properties. Differences in morphological and photocatalytic properties between the samples synthesized by the PC and SSR methods were also clarified.

2. Experimental section

2.1 Chemicals

Zinc nitrate hexahydrate ($Zn(NO_3)_2 \cdot 6H_2O$, 99%), copper nitrate trihydrate ($Cu(NO_3)_2 \cdot 3H_2O$, 99%), ethylenediamine (EDA) and nitric acid (HNO_3) were purchased from Kanto Chemical. Anhydrous citric acid (CA, 98%) was purchased from Wako Pure Chemical. Gallium metal (Ga, 99.99%), zinc sulfide (ZnS, 99.999%), copper (I) sulfide (Cu_2S, 99%) and gallium sulfide (Ga_2S_3, 99.999%) were purchased from Kojundo Chemical. All chemicals were used as received. An aqueous solution of gallium nitrate ($Ga(NO_3)_3$, 1.00 mol L^{-1}) was prepared by dissolving gallium in concentrated HNO_3, the excess of nitric acid was removed by evaporation. Distilled water was used for experiments.

2.2 Synthesis of $Zn_{1-2x}(CuGa)_xGa_2S_4$ *via* PC method

Powders of $Zn_{1-2x}(GuGa)_xGa_2S_4$ were synthesized by sulfurization of oxide precursors with corresponding composition for metals. Oxide precursors were prepared by a PC method. CA was added to an aqueous solution containing metal nitrates according to stoichiometry. After stirring at 353 K for a period of 3 hours to form CA-metal complexes, the temperature was raised to 403 K followed by the addition of EDA to achieve polyamidation reaction between CA and EDA. Although glycols are generally used in the PC method to achieve esterification between CA and glycols,[46] a precipitate of Cu(I)-glycol complex appeared when a solution containing copper ions and ethylene glycol or propylene glycol was heated. Therefore, EDA was used as polymerization reagent instead of glycols to achieve a homogeneous process. The ratio of metal: CA:EDA was 1:4:8. After several hours of stirring, a highly viscous matter was obtained, which was then pyrolysed in air by increasing gradually the temperature to 823 K, resulting in the oxide precursor. Precursors for different compositions were prepared changing the ratio of metal nitrates according to the chemical formula of $Zn_{1-2x}(GuGa)_xGa_2S_4$ with 0.1 step in x. The precursors were heat-treated under a H_2S (10%)-Ar flow (20 mL min^{-1}) using a tubular furnace at 1173 K for a period of 5 hours to sulfurize precursor. After cooling down to room temperature, the final samples were gently ground and characterized. $Zn_{0.4}(CuGa)_{0.3}Ga_2S_4$ (x = 0.3) was also prepared as a reference sample by the SSR method according to the previous report.[40] Powders of ZnS, Cu_2S, and Ga_2S_3 were mixed in a stoichiometric ratio. The mixture was then sealed in a quartz ampoule tube under vacuum, and heat-treated at 1023 K for a period of 8 hours.

2.3 Characterization

Crystal phases of the samples were identified by powder X-ray diffraction (XRD) technique using Cu Kα radiation (Bruker AXS, D2 Phaser). Ultraviolet-visible (UV-vis) spectra were collected by a UV-Vis diffuse reflection spectrometer with an integrating sphere (Shimadzu, UV-3100), followed by the Kubelka-Munk transformation method. The samples were observed by scanning electron microscopy (SEM; Hitachi, S-4800). The specific surface areas were determined by the Brunauer-Emmet-Teller method (Micromeritics, ASAP 2010). Surface composition was analyzed by X-ray photoelectron spectroscopy (XPS; Kratos, ESCA-3400). The elemental composition of the samples was determined by inductively coupled plasma atomic emission spectroscopy (ICP-AES; SPECTRO, SPECTRO ARCOS).

2.4 Evaluation of photocatalytic activity

Evaluation of the photocatalytic activity was conducted using a gas-flow system coupled to an on-line gas chromatograph (Agilent Technologies, micro GC 490). Photocatalyst (0.30 g) was dispersed in 150 mL of water containing Na_2S (0.1 mol L^{-1}) and Na_2SO_3 (0.5 mol L^{-1}) of sacrificial reagents to avoid photocorrosion. Cocatalysts (Ru, Rh and Pd) were photodeposited along with the measurement by addition of proper amounts of $RuCl_3$, $Rh(NO_3)_3$ and $PdCl_2$ to the reactant solution. Photocatalysts were irradiated with visible light (λ > 420 nm) by a 300-W Xe lamp (Excelitas, Cermax PE300BF) with a cut-off filter. The photocatalyst was collected by a centrifugal method after 5 hours of H_2 evolution. A second cycle of H_2 evolution was then examined using the collected sample and a fresh reactant solution to check the recycle stability. For the measurement of apparent quantum yields, a monochromatic light of 420 nm (Asahi Spectra, MAX-303) was used.

3. Results and discussion

3.1 Synthesis and characterization

Colour of oxide precursors was black except for x = 0 containing no Cu. It suggested that the oxidation state of Cu in the precursors was not Cu(I) but Cu(II) since those were obtained by pyrolysis in air. Fig. 1 shows XRD patterns of oxide precursors with different compositions prepared by the PC method. All precursors were assigned to spinel-type compound while the crystallinity decreased as contents of Cu and Ga increased. Formation of spinel phase is reasonable for x = 0 because zinc gallium oxide with a ratio Zn:Ga = 1:2 regularly crystallizes in a spinel phase $ZnGa_2O_4$. It should be noticed that the precursors with x = 0.1–0.5 were also spinel phases with low crystallinity although the phase separation into spinel-compound $(Cu,Zn)Ga_2O_4$ and Ga_2O_3 with detectable contents (>10 wt%) was expected from the composition. Besides, decreases in crystallinity of the spinel phase with increasing the substitution are reasonable for the formation of the spinel phase with defects at the Zn site. The facts of no appearance of Ga_2O_3 and the decreasing crystallinity in the precursors indicate homogeneous distribution of the constituent elements in the precursors obtained by the PC method. This is a preferable characteristic for the precursors to be converted to complex sulfides by sulfurization. Fig. 2 shows XRD patterns of $Zn_{1-2x}(CuGa)_xGa_2S_4$ synthesized from the oxide precursors. Diffraction patterns of all samples were attributed to the defect chalcopyrite phase with high crystallinity. No appearance of Ga_2O_3 phase is an improvement over the samples synthesized by the SSR method, in which Ga_2O_3 is observed due to the partial hydrolysis of Ga_2S_3.[40] Two phenomena were seen in XRD analysis for the PC samples tracing the previous report on the SSR samples. Some diffraction peaks shifted to higher angles owing to difference in the ionic size between substituents (Cu^+: 0.060 nm and Ga^{3+}: 0.047 nm) and Zn^{2+} (0.060 nm) with increasing substitution. The splits between (220) and (024), and between (132) and (116)

reflections observed around 49º and 58º, respectively, deceased gradually due to getting more symmetric structure with increasing substitution. These results clearly proven the successful synthesis of $Zn_{1-2x}(GuGa)_xGa_2S_4$ in all desired compositions *via* the PC method. In addition, XPS of Cu 2p showed a single sharp peak at 935 eV and no satellite peaks around 945 eV, indicating the oxidation state of Cu was +1 (Fig. S1).

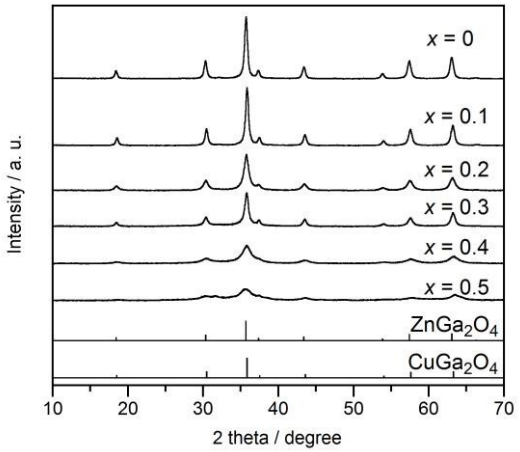

Fig. 1 XRD patterns of oxide precursors prepared by the PC method. Reference patterns of $ZnGa_2O_4$ and $CuGa_2O_4$ are also presented.

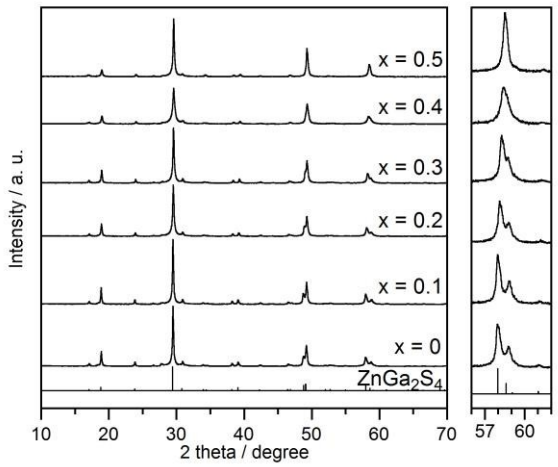

Fig. 2 XRD patterns of $Zn_{1-2x}(CuGa)_xGa_2S_4$ synthesized by sulfurization of oxide precursors prepared by the PC method. Reference pattern of $ZnGa_2S_4$ is also presented.

Fig. 3 shows UV-vis spectra of $Zn_{1-2x}(CuGa)_xGa_2S_4$. While $ZnGa_2S_4$ has a wide band gap of 3.4 eV with an absorption edge in the UV region, even small amount of substitution for $ZnGa_2S_4$ causes a remarkable red shift in the absorption edge, resulting in the absorption in the visible light. With increasing substitution, the absorption edge suffered a red shift until $CuGa_5S_8$ (x = 0.5) was obtained. Previous study has reported that the band gaps are affected both by Cu^+ and Ga^{3+}.[40] Even though the remarkable red shift observed is mainly due to a raise in the VB with the contribution of Cu 3d orbital, there is also lowering the potential of the CB owing to the decrease in the contribution of Zn 4s4p.

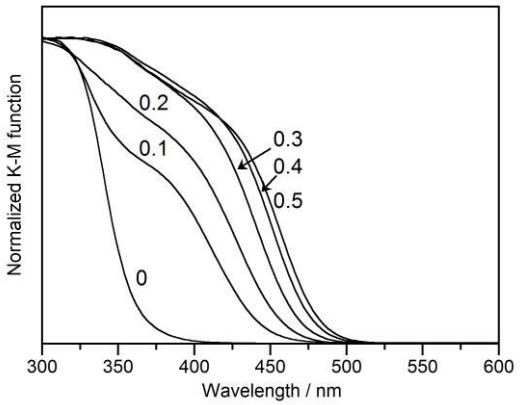

Fig. 3 UV-vis spectra of $Zn_{1-2x}(CuGa)_xGa_2S_4$ with given compositions.

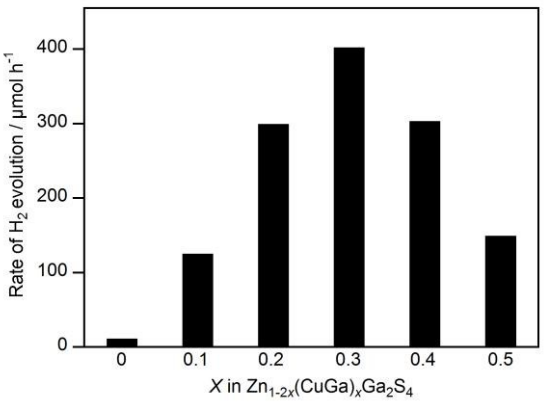

Fig. 4 Rates of H_2 evolution for Rh(1.0 wt%)/$Zn_{1-2x}(CuGa)_xGa_2S_4$ photocatalysts under visible light irradiation. Reactant solution contained Na_2S (0.1 mol L^{-1}) and Na_2SO_3 (0.5 mol L^{-1}) as sacrificial reagents.

Fig. 4 shows photocatalytic activity of Rh(1.0 wt%)-loaded $Zn_{1-2x}(CuGa)_xGa_2S_4$ synthesized *via* the PC method for H_2 evolution from an aqueous solution containing Na_2S and Na_2SO_3 under visible light. All samples containing Cu produced H_2 while $ZnGa_2S_4$ (x = 0) was almost inactive due to the lack of absorption of visible light. With increasing amount of substitution, the activity was enhanced until $Zn_{0.4}(CuGa)_{0.3}Ga_2S_4$ (x = 0.3), however, the activity decreased with further substitution. Thus, $Zn_{0.4}(CuGa)_{0.3}Ga_2S_4$ was the most active composition. This is the same result as that the series of the SSR samples shows.[40] It is stressed that the most active composition is $Zn_{0.4}(CuGa)_{0.3}Ga_2S_4$ as an intrinsic feature in the $Zn_{1-2x}(CuGa)_xGa_2S_4$ system irrespective of the synthesis methods. Increasing substitution offers both of positive and negative effects reflecting their band structures upon photocatalytic H_2 evolution as reported for the SSR sample.[40] The positive effect, which is mainly brought by increasing the contents of Cu, is narrowing band gaps which allows the increase in number of available photons. The negative one is the decrease in driving force for reduction of water by lowering potential of CB owing to the decrease in the contents of Zn as described above. The negative factor becomes significant beyond x = 0.3, and suppresses H_2 evolution significantly. The composition is a dominant factor determining the band structure of the solid solution rather than synthesis methods. Therefore, the highest activity is obtained intrinsically at x = 0.3 for both PC and SSR samples.

3.2 Comparing properties of $Zn_{0.4}(CuGa)_{0.3}Ga_2S_4$ synthesized by PC and SSR methods

Synthesis of materials by different methods often varies their properties. Fig. 5 shows the XRD patterns of $Zn_{0.4}(CuGa)_{0.3}Ga_2S_4$ prepared by PC and SSR methods. As previously mentioned, the PC sample had the advantage of no presence of a Ga_2O_3 impurity against the SSR sample. When analysing the intensity and sharpness of the diffraction peaks, the SSR sample exhibited higher intensity and narrower peak widths than the PC sample, even though the sulfurization temperature for the PC method (1173 K) was 150 K higher than synthesis temperature for SSR (1023 K). This suggested that smaller particles were obtained by the PC method in comparison with the SSR method. Absorption edges in UV-vis spectra of $Zn_{0.4}(CuGa)_{0.3}Ga_2S_4$ synthesized by PC and SSR methods were the same (Fig. S2). However, comparing the absorption profile of both samples, it can be noticed that absorption rises steeply in the SSR sample in comparison with the PC sample. It also implies the presence of small particles in the PC sample since the slow increase in absorption in the PC sample would be due to light scattering caused by small particles. To clarify this point, particle observation by SEM was conducted (Fig. 6). Particles in the SSR sample were 1–2 μm in size and possessing smooth surfaces, like as crystal facets, with step-like edges. In contrast, the PC sample were sponge-like aggregates composed of fine particles with 50 nm of the size. The PC samples exhibited type-II of nitrogen adsorption-desorption isotherms with hysteresis attributed to interparticle voids in the aggregates of fine particles, which offered irregular pores in sizes (Fig. S3). The sponge-like morphology in the PC samples was also confirmed from nitrogen adsorption-desorption analysis. Thus, it was proven that morphology of the particles significantly changed by the synthesis method. Formation of intermediates possessing low melting points is possible explanation for the grown particles exposing smooth facets in the SSR sample in spite of the relatively low synthesis temperature. In the PC method, formation of such intermediates giving the fluxing effect may hardly occur, because sulfurization proceeds from the surface of oxide precursor, in which constituents are homogeneously dispersed. It resulted in the aggregates of fine particles in the PC sample. Difference in the particle sizes was reflected in their specific surface areas. The PC samples had a remarkably larger surface area (20.7 $m^2 g^{-1}$) than the SSR sample (1.6 $m^2 g^{-1}$).

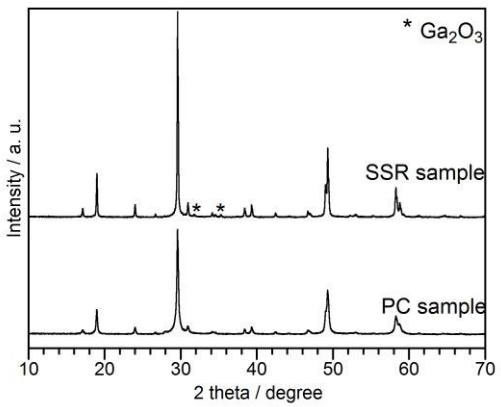

Fig. 5 XRD patterns of $Zn_{0.4}(CuGa)_{0.3}Ga_2S_4$ synthesized by PC and SSR methods.

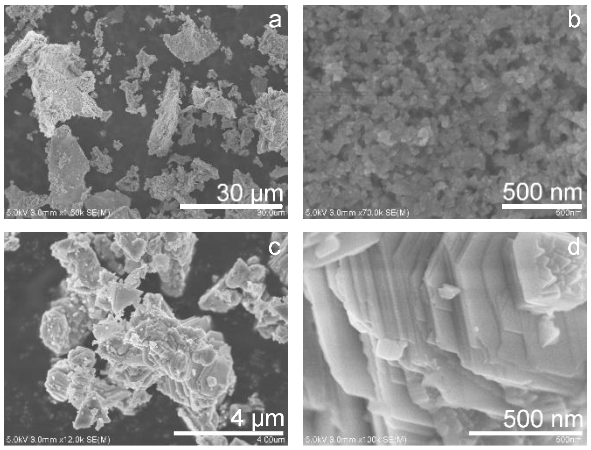

Fig. 6 SEM images of $Zn_{0.4}(CuGa)_{0.3}Ga_2S_4$; (a, b) for the PC sample and (c, d) for the SSR sample.

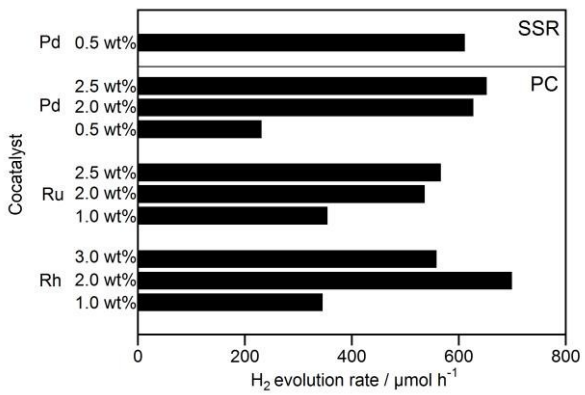

Fig. 7 Photocatalyytic H_2 evolution rates of cocatalyst-loaded $Zn_{0.4}(CuGa)_{0.3}Ga_2S_4$ prepared by the PC and SSR methods.

The SSR sample exhibits the best performance for H_2 evolution with deposition of 0.5 wt% of a Pd cocatalyst.[40] Changes in the optimal conditions of cocatalysts was expected from the significant changes in morphology and particle sizes. Fig. 8 shows activity for H_2 evolution over the PC sample modified with various cocatalysts. Where the activity of the optimized SSR sample modified with a Pd cocatalyst is also presented. The PC sample exhibited high activities when relatively large amounts of cocatalysts were deposited in comparison with the optimal amount of Pd for the SSR sample (0.5 wt%). It is reasonable in consideration of the larger surface areas of the PC sample. The rate of H_2 evolution was improved about 20% by the Rh(2 wt%)-loaded PC sample as compared with the optimized SSR sample. The apparent quantum yield was also improved from 15% to 19% by the synthesis using the PC method. However, this improvement was smaller than that expected from the large surface area. It would be due to suppression of recombination in the SSR sample with low defects owing to the fluxing effect as mentioned above. When we see the cocatalyst dependence, it is noticed that the preferred cocatalyst is different for each sample. It has been reported that the activity of the SSR sample depends on the kinds of cocatalysts, and the order of activity is Rh < Ru < Pd. The order of activity for the PC sample, Ru < Pd < Rh, was different from that for the SSR sample. The surface properties are being important factors for photocatalysts because that the surfaces

provide not only reaction sites for oxidation reaction but also interfaces between photocatalysts and cocatalysts. The XPS analysis revealed that there were no remarkable differences in the elemental composition at the surface between the PC and SSR samples (Table 1). Moreover, the surface composition was well consistent with the bulk composition analyzed by ICP-AES. Therefore, it is concluded that morphological properties owe to the differences in the effective cocatalysts observed.

Table 1 Elemental analysis by ICP-AES and XPS for $Zn_{0.4}(CuGa)_{0.3}Ga_2S_4$ synthesized by the PC and SSR method

sample	analysis method	composition (atom%)		
		Cu	Ga	Zn
Ideal	-	10.0	76.7	13.4
PC	ICP-AES	10.1	77.0	12.7
PC	XPS	13.7	73.1	13.2
SSR	ICP-AES	10.5	76.9	12.2
SSR	XPS	13.8	73.7	12.4

As described above, it has been revealed that the PC sample has higher performance than the SSR sample. Finally, the recycle stability of the PC sample was examined. Fig. 8 represents the time course of H_2 evolution using Rh(2 wt%)-loaded $Zn_{0.4}(CuGa)_{0.3}Ga_2S_4$ synthesized by the PC method with intermediate collection of the sample after 5 hours of irradiation. The sample steadily produced H_2 without degradation even in the second cycle. Thus, good recycle stability of Rh-loaded $Zn_{0.4}(CuGa)_{0.3}Ga_2S_4$ was proven. Total amount of H_2 produced for 5 hours of irradiation in the second run was slightly larger than that in the first cycle. It is because the absence of the induction period for deposition of the Rh cocatalyst in the second cycle.

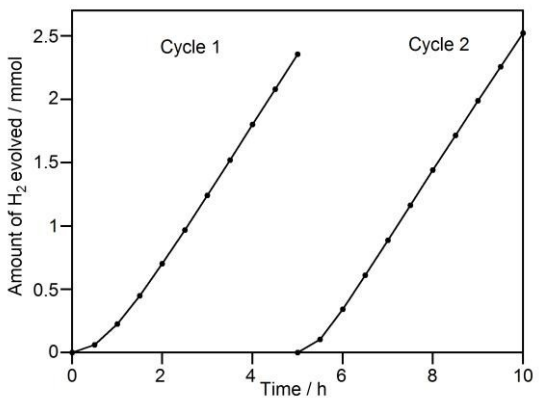

Fig. 8 Time course of H_2 evolution over Rh(2 wt%)-loaded $Zn_{0.4}(CuGa)_{0.3}Ga_2S_4$ under visible light with intermediate collection of the sample.

4. Conclusion

The morphology of $Zn_{1-2x}(CuGa)_xGa_2S_4$ synthesized by sulfurization of the oxide precursor obtained by the PC method was rather different from that of the SSR sample. The PC samples were aggregates of fine particles with 50 nm of size, having a large specific surface area (20.7 $m^2\ g^{-1}$), whereas the particles in the SSR were grew about 1–2 μm in size, and exposed smooth surfaces. It has been demonstrated that the synthesis method changes the morphology of the $Zn_{1-2x}(CuGa)_xGa_2S_4$ particle, and that the present synthesis method is useful to obtain fine particles of $Zn_{1-2x}(CuGa)_xGa_2S_4$. Accordingly, an improvement in the efficiency for H_2 evolution from aqueous solution containing sacrificial reagents from 15% (the SSR sample) to 19% has been achieved. It has been also predicted that smooth surfaces with low defects is also effective factor for this photocatalyst.

Acknowledgements

This research was supported by a Grain-in-Aid (No. 24107004) for Innovative Areas (Area No. 2406) from MEXT, Japan.

Notes and references

[a] Institute of Multidisciplinary Research for Advanced Materials, Tohoku University, 2-1-1 Katahira, Aoba-ku, Sendai, Miyagi 980-8577, Japan. E-mail: hkato@tagen.tohoku.ac.jp
[b] Department of Applied Chemistry, Faculty of Science, Tokyo University of Science, 1-3 Kagurazaka, Shinjuku-ku, Tokyo 162-8601, Japan
[c] Photocatalysis International Research Center, Research Institute for Science and Technology, Tokyo University of Science, Japan

1 A. Fujishima, K. Honda, *Nature*, 1972, **238**, 37.
2 A. Kudo, Y. Miseki, *Chem. Soc. Rev.*, 2009, **38**, 253.
3 R. Abe, J. *Photochem. Photobiol. C*, 2010, **11**, 179.
4 S. Linic, P. Christopher, D. B. Ingram, *Nat. Mater.*, 2011, **10**, 911.
5 Y. Tachibana, L. Vayssieres, J. R. Durrant, *Nat. Photonics*, 2012, **6**, 511.
6 A. Valdés, J. Brillet, M. Grätzel, H. Gudmundsdóttir, H. A. Hansen, H. Jónsson, P. Klüpfel, G. Kroes, F. L. Formal, I. C. Man, R. S. Martins, J. K. Nørskov, J. Rossmeisl, K. Sivula, A. Vojvodic, M. Zäch, Phys. *Chem. Chem. Phys.*, 2012, **14**, 49.
7 V. Preethi, S. Kanmani, *Mater. Sci. Semicond. Process.*, 2013, **16**, 561.
8 X. Li, J. Yu, J. Low, Y. Fang, J. Xiao, X. Chen, *J. Mater. Chem. A*, 2015, **3**, 2485.
9 H. Kato, K. Asakura, A. Kudo, *J. Am. Chem. Soc.*, 2003, **125**, 3082.
10 Y. Sakata, Y. Matsuda, T. Nakagawa, R. Yasunaga, H. Imamura, K. Teramura, *ChemSusChem*, 2011, **4**, 181.
11 X. Chen, S. Shen, L. Guo, S. S. Mao, *Chem. Rev.*, 2010, **110**, 6503.
12 J. Yoshimura, Y. Ebina, J. Kondo, K. Domen, A. Tanaka, *J. Phys. Chem.*, 1993, **97**, 1970.
13 H. Kato, A. Kudo, *J. Phys. Chem. B*, 2002, **106**, 5029.
14 R. Konta, T. Ishii, H. Kato, A. Kudo, *J. Phys. Chem. B*. 2004, **108**, 8992.
15 H. G. Kim, D. W. Hwang, J. S. Lee, *J. Am. Chem. Soc.*, 2004, **126**, 8912.
16 R. Niishiro, H. Kato, A. Kudo, *Phys. Chem. Chem. Phys.*, 2005, **7**, 2241.
17 S. K. Biswas, J. B, B. B. Kale, R. K. Yadav, S. Moon, K. Kong, W. So, *Catal. Commun.*, 2011, **12**, 651.
18 R. Asai, H. Nemoto, Q. Jia, K. Saito, A. Iwase, A. Kudo, *Chem. Commun.*, 2014, **50**, 2543.
19 M. Liu, W. You, Z. Lei, G. Zhou, J. Yang, G. Wu, G. Ma, G. Luan, T. Takata, M. Hara, K. Domen, C. Li, *Chem. Commun.*, 2004, **19**, 2192.
20 M. Liu, W. You, Z. Lei, T. Takata, K. Domen, C. Li, *Chin. J. Catal.*, 2006, **27**, 556.

21 T. Hisatomi, K. Maeda, K. Takanabe, J. Kubota; K. Domen, *J. Phys. Chem. C*, 2009, **113**, 21458.
22 K. Maeda, M. Higashi, D. Lu, T. Takata, R. Abe, K. Domen, *J. Am. Chem. Soc*., 2010, **132**, 5858.
23 X. Wang, K. Maeda, A. Thomas, K. Takanabe, G. Xin, J. M. Carlsson, K. Domen, M. Antonietti, *Nat. Mater*., 2009, **8**, 76.
24 L. Ge, F. Zuo, J. Liu, Q. Ma, C. Wang, D. Sun, L. Bartels, P. Feng, *J. Phys. Chem. C*, 2012, **113**, 13708.
25 S. Cao, J. Yu, *J. Phys. Chem. Lett.*, 2014, **5**, 2101.
26 A. Kudo, I. Tsuji, H. Kato, *Chem. Commun*., 2002, **17**, 1958.
27 I. Tsuji, H. Kato, H. Kobayashi, A; Kudo, *J. Am. Chem. Soc.*, 2004, **126**, 13406.
28 I. Tsuji, H. Kato, A. Kudo, *Angew. Chem. Int. Ed.*, 2005, **44**, 3565.
29 I. Tsuji, H. Kato, H. Kobayashi, A. Kudo, *J. Phys. Chem. B*, 2005, **109**, 7323.
30 I. Tsuji, H. Kato, A. Kudo, *Chem. Mater*., 2006, **18**, 1969.
31 J.S. Jang, D.W. Hwang, J.S. Lee, *Catal. Today*, 2007, **120**, 174.
32 I. Tsuji, Y. Shimodaira, H. Kato, H. Kobayashi, A. Kudo, *Chem. Mater*., 2010, **22**, 1402.
33 H. Kaga, K. Saito, A. Kudo, *Chem. Commun.*, 2010, **46**, 3779.
34 M. Tabata, K. Maeda, T. Ishihara, T. Minegishi,m T. Takata, K. Domen, *J. Phys. Chem. C*, 2010, **114**, 11215.
35 O. M. Saad, T. Kuzuya, S. Hirai, M. Ohta, *Mater. Trans.*, 2010, **51**, 2289.
36 M. Kimi, L. Yuliati, M. Shamsuddin, *Int. J. Hydrogen Energy*, 2011, **36**, 9453.
37 V. Preethi, S. Kanmani, *Int. J. Hydrogen Energy*, 2012, **37**, 18740.
38 X. An, J. C. Yu, F. Wang, C. Li, Y. Li, *Appl. Catal. B*, 2013, **129**, 80.
39 P. C. Lin, P. Y. Wang, Y. Y. Li, C. C. Hua, T. C. Lee, *Int. J. Hydrogen Energy*, 2013, **38**, 8254.
40 H. Kaga, A. Kudo, *J. Catal.*, 2014, **310**, 31.
41 S. Chen, X. Chen, Q. Jiang, J. Yuan, C. Lin, W. Shanguan, *Appl. Surf. Sci.*, 2014, **316**, 590.
42 X. Chen, W. Chen, H. Gao, Y. Yang, W. Shangguan, *Appl. Catal. B*, 2014, **152**, 68.
43 J. Li, L. Wu, L. Long, M. Xi, X. Li, *Appl. Surf. Sci.*, 2014, **322**, 265.
44 H. Wang, W. Chen, J. Zhang, C. Huang, L. Mao, *Int. J. Hydrogen Energy*, 2015, **1**, 340
45 Q. Li, H. Meng, P. Zhou, Y. Zheng, J. Wang, J. Yu, J. Gong, *ACS Catal.*, 2013, **3**, 882.
46 S. Ikeda, M. Hara, J. N. Kondo, K. Domen, H. Takahashi, T. Okubo, M. Kakihana, *Mater. Chem.*, 1998, **10**, 72.
47 Q. Chen, C. Suo, S. Zhang, Y. Wang, *Int. J. Photoenergy*, 2013, **2013**, 1.
48 L. Yuliati, M. Kimi, M. Shamsuddin, Beilstein *J. Nanotechnol.*, 2014, **5**, 587.
49 L. Wang, L. Chen, T. Luo, Y. Qian, *Mater. Lett.*, 2006, **60**, 3627.
50 S. Shen, L. Zhao, L. Guo, *J. Phys. Chem. Solids*, 2008, **69**, 2426.
51 M. Dai, S. Ogawa, T. Kameyama, K. Okazaki, A. Kudo, S. Kuwabata, Y. Tsuboi, T. Torimoto, *J. Mater. Chem.*, 2012, **22**, 12851.

Table of Contents Entry

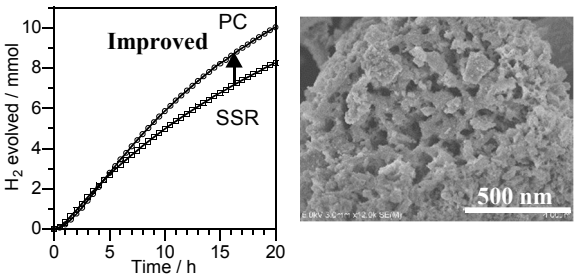

Improvement of photocatalytic activity of $Zn_{1-2x}(CuGa)_xGa_2S_4$ has been realized by sponge-like porous particles composed of 50 nm of fine crystals, which were synthesized by a novel two-step route.